Available online at www.sciencedirect.com
SCIENCE DIRECT®
ELSEVIER
Journal of Petroleum Science and Engineering 40 (2003) 145–157
JOURNAL OF PETROLEUM SCIENCE & ENGINEERING
www.elsevier.com/locate/petrol

Estimation of shale volume using a combination of the three porosity logs

Mostafa H. Kamel*, Walid M. Mabrouk

Geophysics Department, Faculty of Science, Cairo University, Giza, Egypt

Accepted 20 May 2003

Abstract

An equation was developed for evaluating the volume of shale using standard porosity logs such as neutron, density and acoustic logs. The equation is written in terms of several parameters that are readily available from well-log measurements. This equation, which takes into consideration the effect of matrix, fluid and shale parameters, applies reasonably well for many shaly formations independent of the distribution of shales. The results demonstrate the applicability of the equation to well-log interpretation as a procedure for computing shale volume in shaly sand sedimentary sections.

Three key advantages of the proposed equation are: (1) it incorporates several parameters that directly or indirectly affect the determination of shale in one equation, (2) it integrates the three porosity tools for a more accurate determination, and (3) it works well in hydrocarbon-bearing formations and where radioactive material other than shale is present.

Successful application of the equation to shaly sand reservoirs is illustrated by analyses of samples from the Gulf of Suez.

Keywords: Shale volume determination; Sonic–density–neutron and shaly relationship; Influence of the three porosity tools on shale evaluation; An equation for computing shale volume

1. Introduction

An essential step in the formation evaluation process is the determination of the amount of shale present in the formation because it is necessary to calculate formation porosity and fluid content. The presence of shale in a porous-permeable formation, if not accounted for, will normally cause the calculation of a neutron or acoustic derived porosity to be optimistic and may affect the behavior of all logs. Also, porosity calculated from the density device will be optimistic, except when the shale density is greater than the clean matrix density. If the shale density is greater than the clean matrix density, the calculated porosity will be pessimistic.

Today, several log-derived clay content (shaliness) indicators are normally employed for the determination of shaliness, which are derived from single logs (gamma ray, neutron, resistivity, or self-potential) or a combination of two logs (density–neutron, neutron–acoustic). By using as many indicators as possible, reliable evaluation of shale is obtained. Excellent reviews of shaly formation analyses have been presented by Worthington (1985) and Fertl (1987).

Each of the indicators may give either the actual value of shale content or an upper limit of that value.

* Corresponding author.
E-mail address: mhk_kamel@yahoo.com (M.H. Kamel).

0920-4105/$ - see front matter
doi:10.1016/S0920-4105(03)00120-7

The minimum among these upper limits is a good approximation of shale content (Poupon and Gaymard, 1970; Ransom, 1977). The final value should be corrected using one of the methods introduced by Clavier et al. (1971), Steiber (1973), or Dresser Atlas (1979). Accordingly, the rock can be differentiated as clean if $V_{sh} < 10\%$; shaly if V_{sh} ranged from 10% to 33% and if the V_{sh} is more than 33%, it is considered to be shale (Table 1).

In order to evaluate the type of shale, whether effective (montmorillonite and illite) or noneffective (kaolinite and chlorite), the log analyst has to compute what is known as the cation exchange capacity (CEC). This parameter, which is defined as the amount of positive ion substitution that takes place per unit weight of dry rock, can be estimated via the equation adopted by Waxman and Smits (1968). Table 1 concludes the abovementioned discussions about the process of shale evaluation.

The determination of reservoir quality in terms of petrophysical parameters, lithology identification, porosity, type and distribution of reservoir fluids, formation permeability and anticipated water cut estimates, is based mainly on the evaluation of shale volume (V_{sh}) since these parameters are all of primary importance to the proper evaluation of reservoir potentiality. Therefore, to quantitatively evaluate a formation, one must accurately estimate the amount of shale for porosity and water saturation determination.

2. Effect of shale on wire line-logging

Whenever shale is present in a formation, every wire line-logging device is affected in one way or another. With the gamma ray device, the presence of radioactive minerals other than shale will cause the calculated shale volume to be too high. This is

Table 1
Process of shale evaluation

Shale volume evaluation					
Single logs				Combination of two logs	
SP	Neutron	Gamma ray	Resistivity	Density–neutron	Neutron–acoustic
Shale corrections					
Clavier et al. (1971) $V_{sh} = 1.7 - \sqrt{3.38 - (X + 0.7)^2}$	Steiber (1973) $V_{sh} = 0.5X/(1.5 - X)$	Dresser Atlas (1979) $V_{sh} = 0.33[2^{(2X)} - 1]$			
Classification according to the volume of shale					
Clean $V_{sh} < 10\%$	Shaly $10 < V_{sh} < 33\%$	Shale $V_{sh} > 33\%$			
Shale types					
Clay type	Clay name	Formula	Density (g/cm^3)	CEC (meq/g)	
Effective	Montmorillonite	$(1/2Ca, Na)_{0.7}(Al, Mg, Fe)_4(Si, Al_8O_{20})(OH)_4$	2.12	0.8–1.5	
	Illite	$K_{1-1.5}Al_4(Si_{6.5-7.0}Al_{1.0-1.5}O_{20})(OH)_4$	2.52	0.1–0.4	
Ineffective	Kaolinite	$Al_4(Si_4O_{10})(OH)_8$	2.41	0.03–0.1	
	Chlorite	$(Mg, Al, Fe)_{12}(Si, Al)_8O_{20}(OH)_{16}$	2.77	0.0	
CEC calculation					
Waxman and Smits (1968) $CEC = 10^{(1.9832V_{sh} - 2.4473)}$					

particularly true of radioactive sands and dolomite. The self-potential measurement (Schlumberger, 1969) is another way for determining shale content because the SP curve tends to follow a straight line (shale base line) through shales with excursions from this line normally occurring opposite cleaner permeable formations allowing the SP to be used as a shale indicator. Factors such as SP-noise, R_w–R_{mf} contrast and hydrocarbon content complicate the derivation of shale content from the SP. The use of high salinity drilling fluids restricts the development of a good SP and hence of a valid determination of shale content. In addition, the presence of shale in a formation will cause the resistivity log to record too low a resistivity. Hilchie (1978) notes that the most significant effect of shale in a formation is to reduce the resistivity contrast between oil or gas, and water. The net result is that if enough shale is present in a reservoir, it may be very difficult, or perhaps impossible, to determine if a zone is productive. Hilchie (1978) suggests that for shale to significantly affect log-derived water saturations, shale content must be greater than 10% to 15%.

All the porosity tools (neutron, density, and sonic) will record a porosity that is too high. The neutron log response in a formation is primarily a function of the formation hydrogen content. Since shale contains various amounts of water the neutron porosity in a shaly interval is a function of both shale content and the liquid filled effective porosity. Shale volume calculations in low porosity zones will be accurate while calculation in higher porosity clean intervals will show too much shale. (i.e., the neutron is an excellent clay indicator in tight formations, but neutron porosity is very sensitive to effective porosity and fluid type.) The density tool, on the other hand, does not react strongly to the shale content of most formations; so many like to use the density for a quick look porosity (i.e., it will not record too high a porosity if the density of shale is equal to or greater than the reservoir's matrix density.) Moreover, the presence of shale increases the sonic travel time, and in unconsolidated formations this increase can be very significant.

The *density–neutron* crossplot relies on the density and neutron response in shale to calculate an estimated shale volume. Calculated shale volumes will be too low in gas-bearing intervals. Choice of the clean matrix-fluid line will determine whether shale volumes calculated for minerals other than the assumed clean line mineral will be calculated with too high or too low shale volume values. Neutron and density values must be valid (hole rugosity must be considered) before this shale evaluation technique is used. The *neutron–acoustic* technique is similar to the density–neutron crossplot described above in that a clean matrix-fluid line and shale-fluid line must be chosen so that shale content can be scaled between the two lines. This crossplot is particularly useful in gas-bearing formations with low water saturation. Care should be taken in using this crossplot because shale has a large effect on both the neutron and acoustic values.

3. Mathematical derivation of proposed shale equation

The effective porosity (ϕ_E) of shaly formations can be obtained from the response of any porosity tool. This calculation, however, requires knowledge of total porosity (ϕ_T), shale content (V_{sh}) and shale porosity (ϕ_{sh}). These three parameters are related as follows:

$$\phi_T = V_{sh}\phi_{sh} + \phi_E \tag{1}$$

Eq. (1) allows one to obtain shale content (V_{sh}) if shale porosity (ϕ_{sh}) is available:

$$V_{sh} = \frac{\phi_T - \phi_E}{\phi_{sh}} \tag{2}$$

In very shaly sands the magnitude of V_{sh} is close to 1, and effective porosity (ϕ_E) is close to zero. From

Table 2
Vertical resolution levels of logging tools (after Ruhovets (1990))

Level	Property obtained	Logging tool
High	Shale volume	Dipmeter, microlog, high-frequency dielectric, unfiltered Pe-index
Medium	Shale volume, and the mode of distribution, porosity, Qv, and CEC	Porosity logs: density, neutron, acoustic
Low	Conductivity, resistivity	Induction, laterolog

Table 3
Sonic transit times and bulk density for different matrices used in the evaluation of shale volume formula (Schlumberger, 1972)

Type of lithology	V_{ma} (ft/s)	Δ_{tma} (μs/ft)	ρ_{ma} (g/cm^3)
Sandstone	18,000 to 19,500	55.5 to 51.0	2.65
Limestone	21,000 to 23,000	47.6 to 43.5	2.71
Dolomite	23,000 to 26,000	43.5 to 38.5	2.87
Anhydrite	20,000	50.0	2.90
Salt	15,000	67.0	2.15

Eq. (1) it follows that $\phi_{sh} = \phi_T$ (Tenchov, 1998). Thus, Eq. (2) can be written:

$$V_{sh} = \frac{\phi_T - \phi_E}{\phi_T} \tag{3}$$

The total porosity (ϕ_T), on the other hand, is usually computed from the neutron–density combination as:

$$\phi_{ND} = \frac{\phi_N + \phi_D}{2} \tag{4}$$

where the neutron porosity (ϕ_N) can be measured from neutron logs and the density-derived porosity (ϕ_D) can be computed using the following equation:

$$\phi_D = \left(\frac{\rho_b - \rho_{ma}}{\rho_f - \rho_{ma}}\right) \tag{5}$$

In 1979, Dresser Atlas introduced an equation to correct the density log for the effect of shale:

$$\phi_D = \left(\frac{\rho_b - \rho_{ma}}{\rho_f - \rho_{ma}}\right) - V_{sh}\left(\frac{\rho_{sh} - \rho_{ma}}{\rho_f - \rho_{ma}}\right) \tag{6}$$

Substituting Eq. (6) into Eq. (4), the following is obtained:

$$\phi_{ND} = 0.5\left[\phi_N + \frac{\rho_b - \rho_{ma}}{\rho_f - \rho_{ma}} - V_{sh}\left(\frac{\rho_{sh} - \rho_{ma}}{\rho_f - \rho_{ma}}\right)\right] \tag{7}$$

In fact, Eq. (7) seems to be approximately equal and very close to the total porosity since the effect of shaliness appears only in density rather than neutron.

Table 4
Log evaluation table of cretaceous pictured cliffs sandstone, San Juan Basin, USA

Depth (ft)	ILD (Ω m)	SFL (Ω m)	ϕ_N (%)	ϕ_D (%)	ρ_b (g/cm^3)	Δ_t (μs/ft)	GR API	ϕ_{ND} (%)	V_{sh} GR	V_{sh} Eq. (13)	Diff. (%)
1926	11	16	25	14.5	2.54	87	70	20.4	0.09	0.06	2.80
1928	12	15	27.5	18	2.49	91.11	70	23.2	0.09	0.05	3.41
1930	13	14	26.5	17	2.27	89	64	22.3	0.00	0.02	– 2.10
1932	14	17	24.5	17	2.56	88	72	21	0.11	0.09	1.53
1934	15	19	24.5	16	2.65	89	74	20.7	0.14	0.16	– 2.40
1936	16	20	25	16.5	2.64	89	74	21.2	0.14	0.15	– 1.36
1938	17	20	24	17	2.56	88	72	21.8	0.11	0.09	1.01
1940	17	23	23.5	14.5	2.59	87	72	19.5	0.11	0.11	– 0.09
1942	18	20	24	17.5	2.63	89	74	21	0.14	0.15	– 1.69
1944	15	18	23	17.5	2.63	89	74	20.4	0.14	0.16	– 2.59
1946	14	15	23	16	2.73	89	76	19.8	0.17	0.22	– 5.02
1948	15	17	25.5	17	2.02	95	84	21.7	0.29	0.21	7.38
1950	15	18	23	18.5	2.48	88	70	20.9	0.09	0.05	3.48
1952	14	20	23	16	2.44	86	68	19.8	0.06	0.01	5.04
Maximum									0.29	0.22	7.38
Minimum									0.00	0.001	– 5.02
Average									0.12	0.11	0.67

GR_{max} = 134 API, GR_{min} = 64 API, Δ_{tsh} = 130 μs/ft, ρ_{sh} = 2.7, ρ_{ma} = 2.65, ρ_f = 1.1 g/cm^3, Δ_{tma} = 55.5 μs/ft, Δ_{tf} = 185 μs/ft.

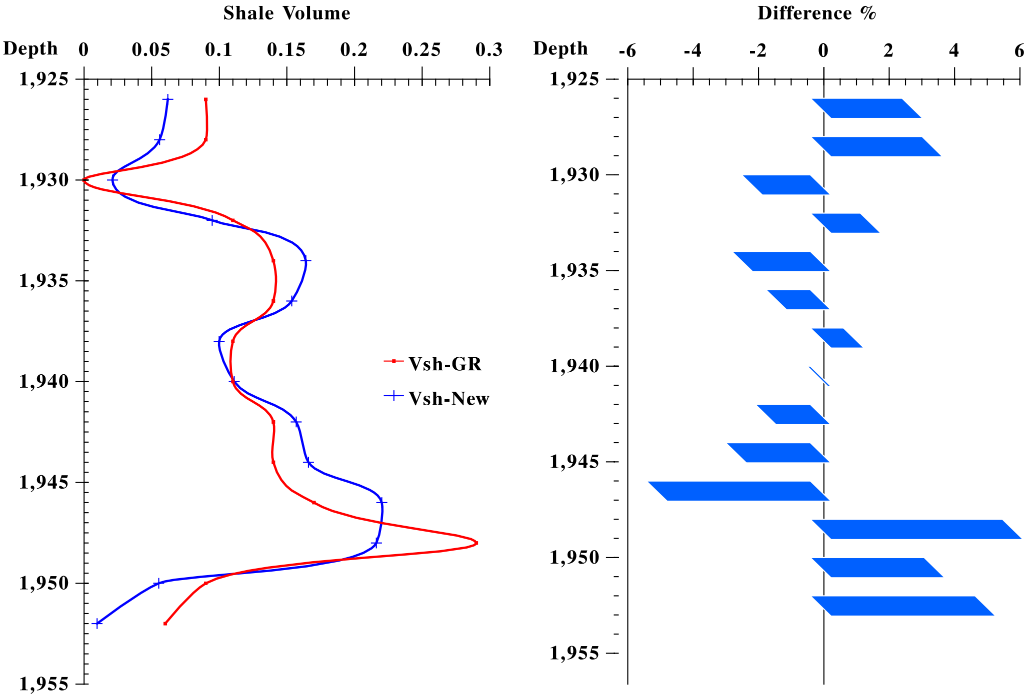

Fig. 1. Comparative look at different shale volume using different approaches. Cretaceous pictured cliffs Sandston, San Juan Basin, USA.

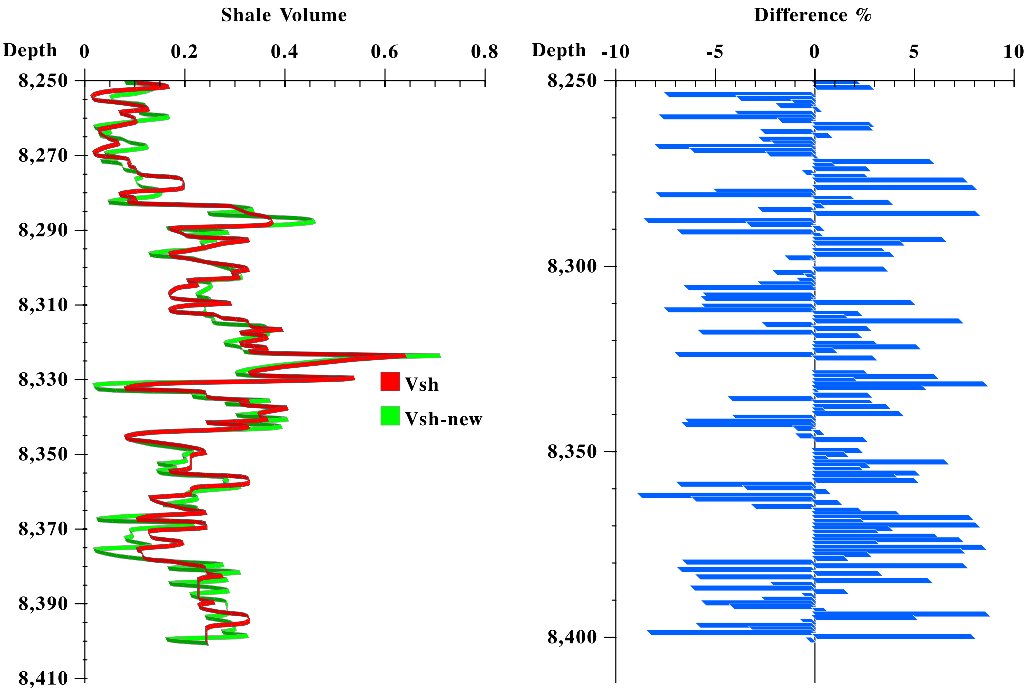

Fig. 2. Comparison of shale volume computed using different approaches with the observed differences, July Oil Field, Gulf of Suez, Egypt.

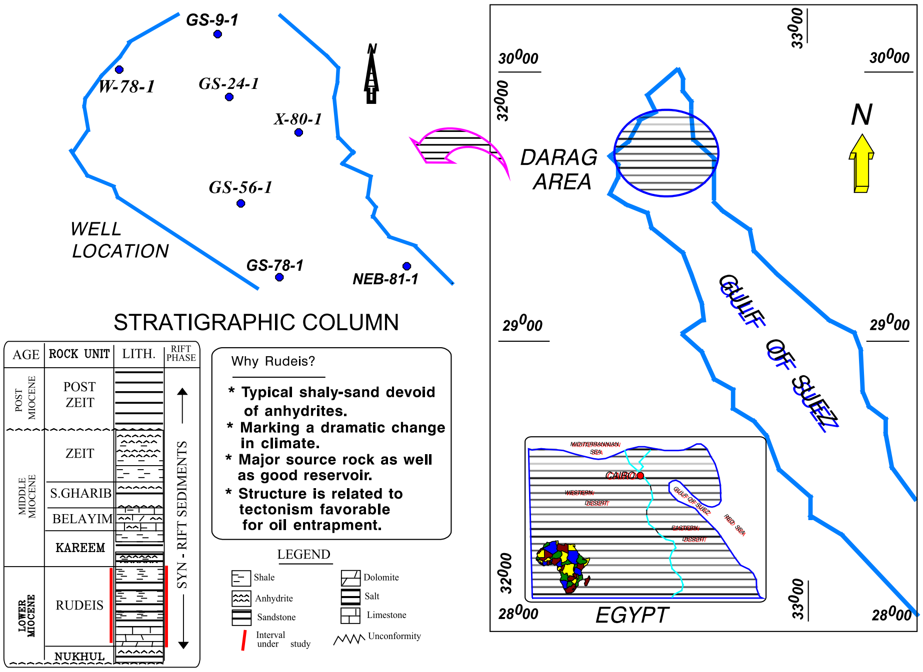

Fig. 3. Location map of the northern portion of the Gulf of Suez, Egypt.

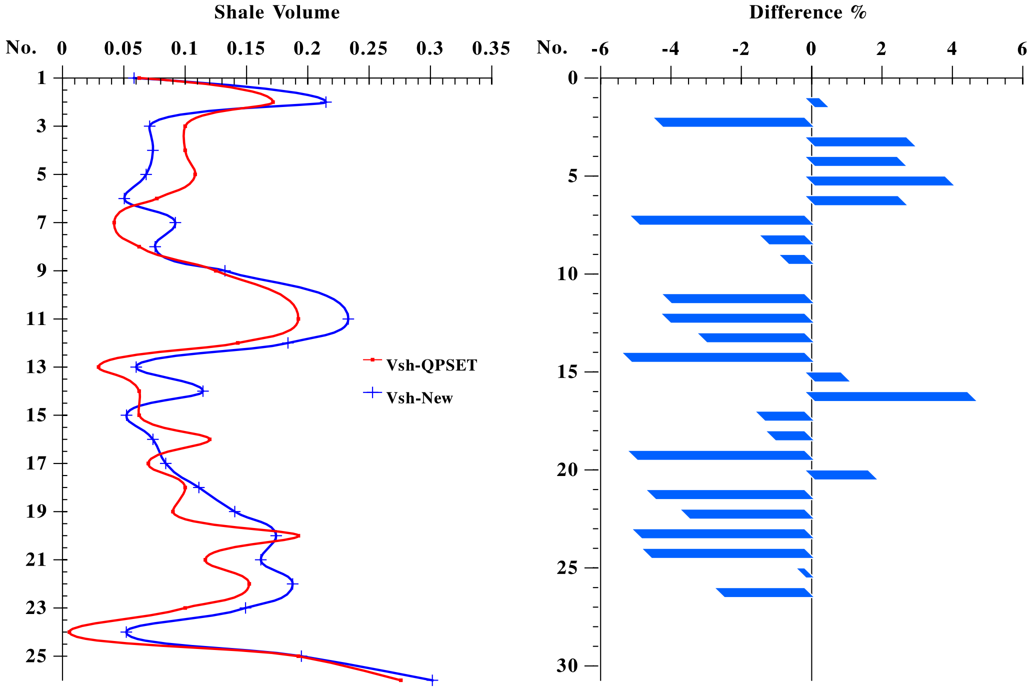

Fig. 4. Comparison of different shale volume computed using QPSET and Eq. (13) with the difference in percentage, Darag Area, Northern Gulf of Suez, Egypt, W78-1.

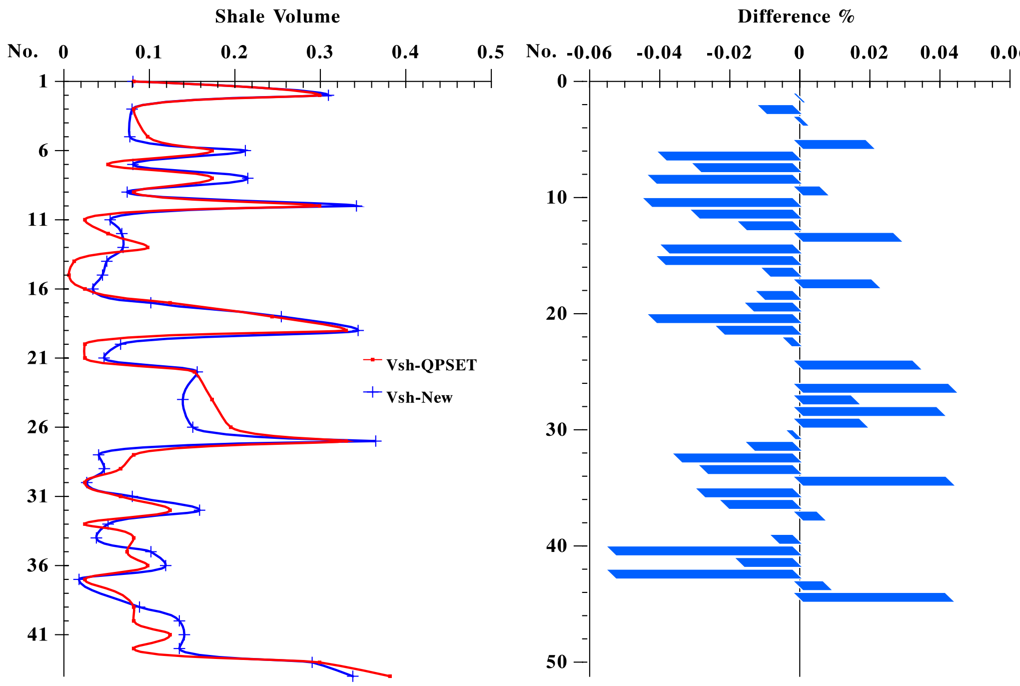

Fig. 5. Comparison of different shale volume computed using QPSET and Eq. (13) with the difference in percentage, Darag Area, Northern Gulf of Suez, Egypt, GS56-1.

Another formula to correct the sonic log for the effect of shaliness was introduced by Dresser Atlas (1979):

$$\phi_S = \left(\frac{\Delta_t - \Delta_{tma}}{\Delta_{tf} - \Delta_{tma}} \times \frac{100}{\Delta_{tsh}}\right) - \left(V_{sh} \times \frac{\Delta_{tsh} - \Delta_{tma}}{\Delta_{tf} - \Delta_{tma}}\right) \tag{8}$$

If we assume that $\phi_E = \phi_S$ and $\phi_T \approx \phi_{ND}$, Eq. (3) can be rewritten as:

$$V_{sh} = 1 - \frac{\phi_S}{\phi_{ND}} \tag{9}$$

Substituting Eqs. (7) and (8) into Eq. (9):

$$V_{sh} = 1 - \frac{2\left(\frac{\Delta_t - \Delta_{tma}}{\Delta_{tf} - \Delta_{tma}} \times \frac{100}{\Delta_{tsh}}\right) - \left(2V_{sh} \times \frac{\Delta_{tsh} - \Delta_{tma}}{\Delta_{tf} - \Delta_{tma}}\right)}{\phi_N + \frac{\rho_b - \rho_{ma}}{\rho_f - \rho_{ma}} - V_{sh}\left(\frac{\rho_{sh} - \rho_{ma}}{\rho_f - \rho_{ma}}\right)} \tag{10}$$

Rearranging Eq. (10), the following second order equation is obtained:

$$\left(\frac{\rho_{sh} - \rho_{ma}}{\rho_f - \rho_{ma}}\right) V_{sh}^2 - \left(\phi_N + \frac{\rho_b - \rho_{ma}}{\rho_f - \rho_{ma}} + \frac{\rho_{sh} - \rho_{ma}}{\rho_f - \rho_{ma}} - 2\frac{\Delta_{tsh} - \Delta_{tma}}{\Delta_{tf} - \Delta_{tma}}\right) V_{sh} + \left(\phi_N + \frac{\rho_b - \rho_{ma}}{\rho_f - \rho_{ma}} - 2\frac{\Delta_t - \Delta_{tma}}{\Delta_{tf} - \Delta_{tma}} \times \frac{100}{\Delta_{tsh}}\right) = 0 \tag{11}$$

which yields an expression of the type

$$Ax^2 + Bx + C = 0 \tag{12}$$

The roots of Eq. (12) are

$$x = \frac{-B \pm \sqrt{B^2 - 4AC}}{2A} \tag{13}$$

where:

$$A=\left(\frac{\rho_{\rm sh}-\rho_{\rm ma}}{\rho_{\rm f}-\rho_{\rm ma}}\right),\ B=-\left(\phi_{\rm N}+\frac{\rho_{\rm b}-\rho_{\rm ma}}{\rho_{\rm f}-\rho_{\rm ma}}+\frac{\rho_{\rm sh}-\rho_{\rm ma}}{\rho_{\rm f}-\rho_{\rm ma}}-2\frac{\Delta_{\rm tsh}-\Delta_{\rm tma}}{\Delta_{\rm tf}-\Delta_{\rm tma}}\right),$$

$$C=\left(\phi_{\rm N}+\frac{\rho_{\rm b}-\rho_{\rm ma}}{\rho_{\rm f}-\rho_{\rm ma}}-2\frac{\Delta_{\rm t}-\Delta_{\rm tma}}{\Delta_{\rm tf}-\Delta_{\rm tma}}\times\frac{100}{\Delta_{\rm tsh}}\right)\ \text{and}$$

$$x=V_{\rm sh}.$$

Eq. (13) incorporates several parameters into one equation for determination of shale volume.

4. Best working conditions of Eq. (13)

1. Since all basic logging tools can be divided into three groups according to their vertical resolution (Table 2), the determination of shale at the medium vertical resolution level (which is intend here) is considered an integral part of density, neutron, and sonic logs.

Most of these porosity tools, specifically density and neutron, are normally affected by several factors such as borehole effect, matrix effect, and environmental conditions including borehole size, temperature/pressure, mud cake thickness, formation and borehole fluid salinities, and mud weight. Hence, corrections of these factors are considered essential before estimating the volume of shale using the equations and charts of Dresser Atlas (1983).

2. The shale density (ρ_{sh}) must not equal matrix density (ρ_{ma}),

3. Hydrocarbon-bearing formations,

4. Matrix is constant, and

5. Radioactive materials other than shale are present.

Moreover, some other parameters included in Eq. (13) must be carefully determined and adjusted. This can be classified into three categories as:

1. Shale parameters: the determination of *shale parameters*, including ρ_{sh} and Δ_{tsh} often depends

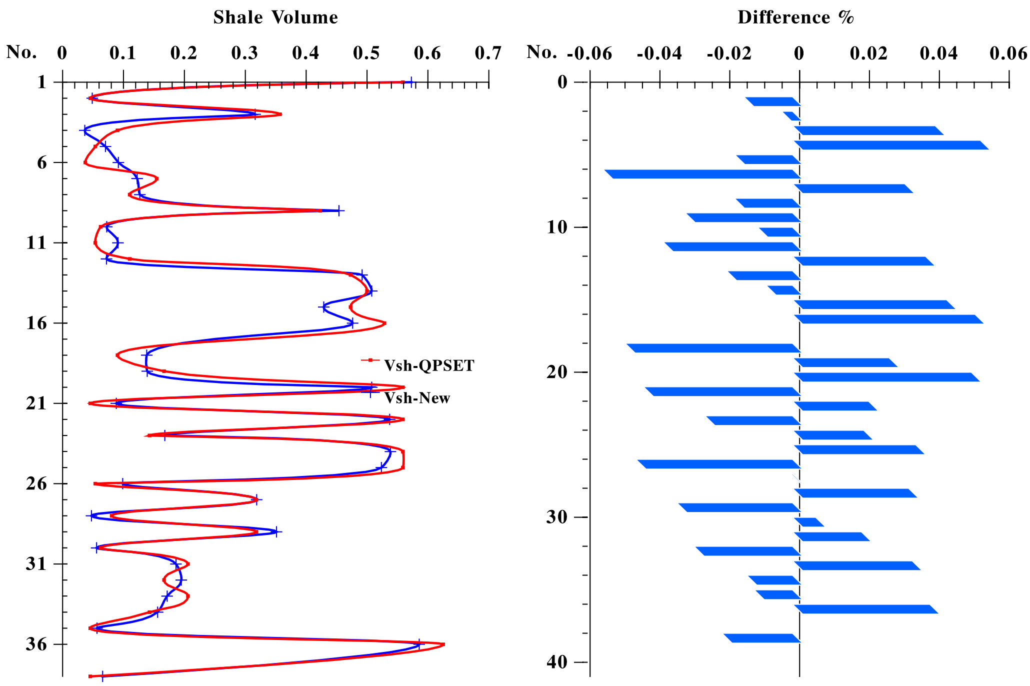

Fig. 6. Comparison of different shale volume computed using QPSET and Eq. (13) with the difference in percentage, Darag Area, Northern Gulf of Suez, Egypt, NEB81-1.

on the experience of the log analyst since such parameters vary according to different geological factors.

2. Matrix parameters: several methods have been outlined by Schlumberger and other service companies to handle the problem of matrix determination such as the M–N plot, MID plot or taken as standard values representing different type of lithology, if known (Table 3).
3. Fluid parameters (ρ_f and Δ_{tf}): these parameters depend mainly on the media either fresh water (ρ_f = 1 g/cm^3 and Δ_{tf} = 189 μs/ft) or saline water (ρ_f = 1.1 g/cm^3 and Δ_{tf} = 185 μs/ft).

5. Validation of the proposed equation

5.1. Cretaceous pictured cliffs Sandston, San Juan Basin, USA

Fortunately, Asquith and Gibson (1982) in their second edition book presented several case studies for evaluating major petrophysical parameters. One of these cases, confined to the Cretaceous Pictured Cliffs sandstone of the San Juan Basin (USA) and representing a shaly sand sedimentary interval (from depth 1926 to 1952 ft), was taken as a test example for Eq. (13). The available log package included in this example helps in estimating shale volume using Eq. (13). This package is in the form of an induction log (DIL) with a spherically focused log (SFL) and an SP log, combination neutron–density (ϕ_{ND}) log (recorded in sandstone porosity units) with a gamma ray log (GR), and density log (ρ_b) with gamma ray log and caliper. A careful examination of the neutron porosity (ϕ_N), density porosity (ϕ_D), and gamma ray log shows that the Cretaceous Pictured Cliffs sandstone is shaly. The shale volume (V_{sh}) was computed from the available gamma ray using the equation adopted by Schlumberger (1975) and corrected by Steiber (1973). Using the available porosity tools (neutron, density and sonic, after being corrected for the previously described effects according to Dresser Atlas, 1983, one can easily apply Eq. (13) to estimate the volume of shale using the parameters indicated on the header of Table 4. The values of shale, after being computed by Eq. (13), are corrected by the same Steiber (1973) equation.

The results obtained are illustrated in Table 4 from which one can easily show that both the Schlumberger (1975) equation and Eq. (13) emphasizing the same lithological zones regardless of observed discrepancies.

Fig. 1, on the other hand, represents the vertical variation of the computed parameter from both approaches with the difference in percentage between them.

6. Field study

A comparison was made using another well, located in the central portion of the Gulf of Suez of Egypt, between the shale volume computed using traditional techniques (i.e., Schlumberger, 1975 and Dresser Atlas, 1979) and Eq. (13) for another test of

Table 5
The calculated minimum, maximum, and average of shale volume using QPSET and Eq. (13), Darag Area, Gulf of Suez, Egypt

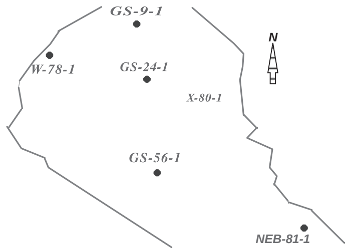

Well name	Location		V_{sh} QPSET	V_{sh} Eq. (13)	Diff. (%)
GS9-1	North	Minimum	0.036	0.013	−0.397
		Maximum	0.147	0.067	9.914
		Average	0.097	0.043	5.382
W78-1	West	Minimum	0.006	0.050	−5.204
		Maximum	0.276	0.302	4.629
		Average	0.110	0.124	−1.429
GS24-1	Center	Minimum	0.143	0.167	−4.436
		Maximum	0.308	0.352	4.603
		Average	0.274	0.276	−0.142
X80-1	East	Minimum	0.007	0.019	−4.742
		Maximum	0.310	0.358	4.032
		Average	0.177	0.173	0.313
GS56-1	Center	Minimum	0.025	0.029	−9.314
		Maximum	0.276	0.242	8.940
		Average	0.155	0.146	0.812
NEB81-1	East	Minimum	0.037	0.036	−5.433
		Maximum	0.625	0.586	5.375
		Average	0.249	0.247	0.206

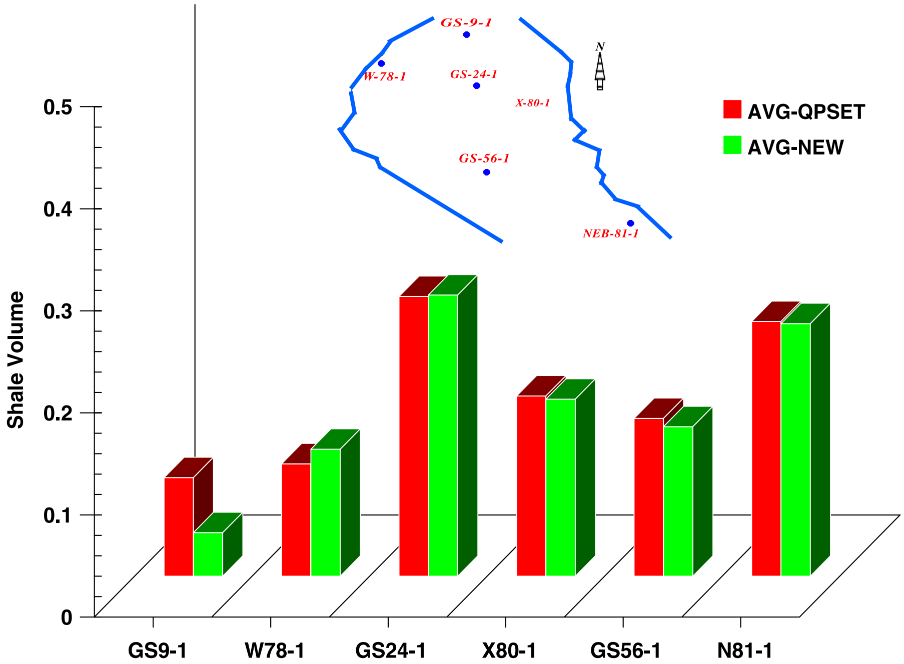

Fig. 7. Histogram of the average values of V_{sh} computed using QPSET and Eq. (13), Darag Area, Gulf of Suez, Egypt.

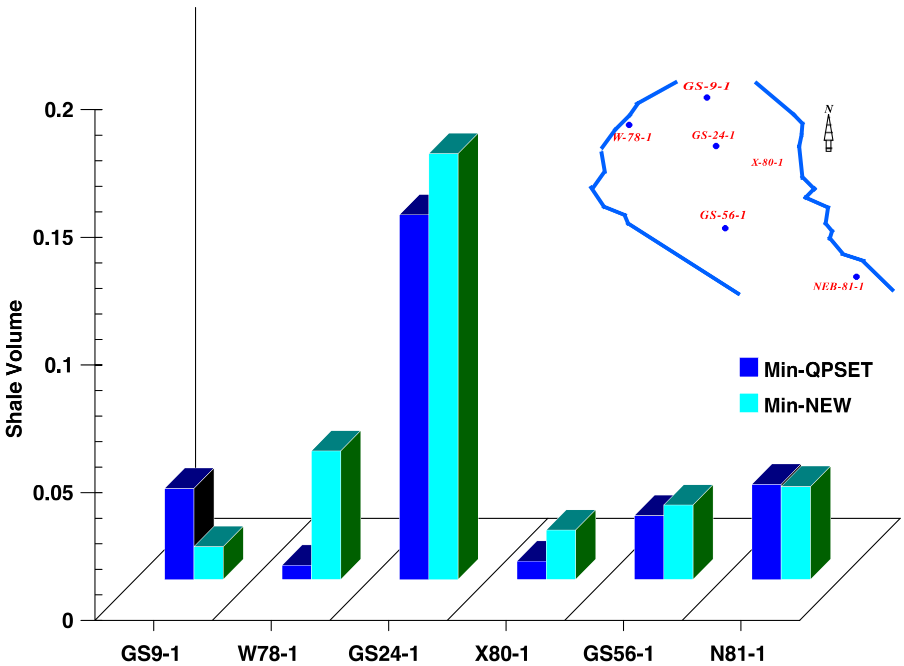

Fig. 8. Histogram of the minimum values of V_{sh} computed using QPSET and Eq. (13), Darag Area, Gulf of Suez, Egypt.

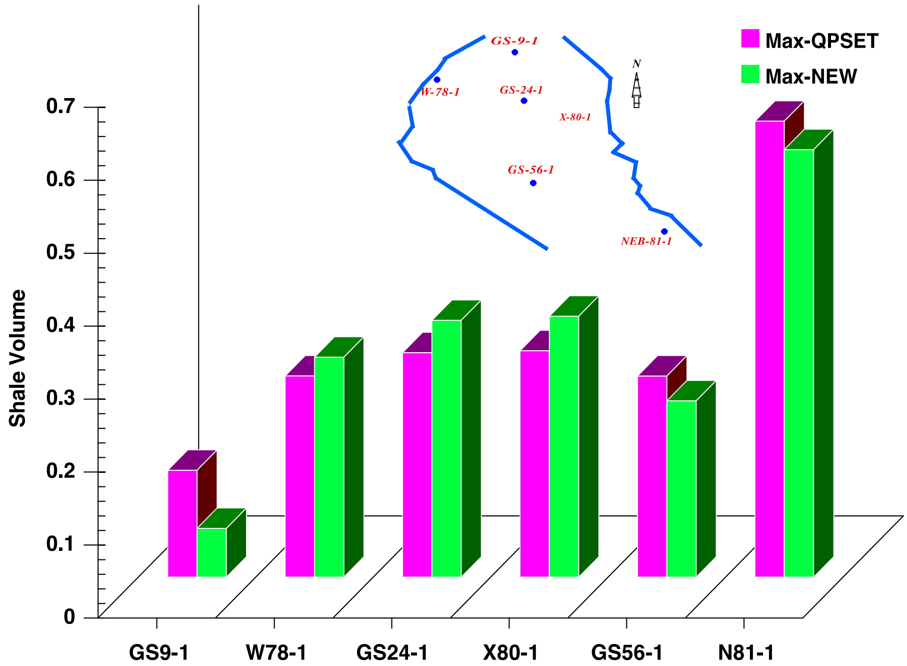

Fig. 9. Histogram of the maximum values of V_{sh} computed using QPSET and Eq. (13), Darag Area, Gulf of Suez, Egypt.

the proposed equation. The Lower Miocene Rudeis formation, from 8250 to 8400 ft, was used. The sequence includes shaly sand with some limestone and a few streaks of dolomite. All data required for Eq. (13), such as standard porosity logs, were available. The results of the comparison illustrated in Fig. 2 show very good agreement.

7. Application

The following discussion is the application of the equation to real field data representing different depths within the thickness range of the Lower Miocene Rudeis sedimentary sections in the six wells located in the Northern Portion of the Gulf of Suez of Egypt, Fig. 3. The choice of these depths is based mainly on the characteristics of the Rudeis formation in the Gulf of Suez. It is considered as a good reservoir and typically consists of shaly sands with few carbonates and no anhydrites. The shale included in this formation is also considered the main source rock.

Fortunately, all input data required to apply Eq. (13) were available and corrected by Kamel et al. (1996) and Abdelrahman et al. (2000) for the area indicated in the same Fig. 3 using a well-based analysis program called “Quantitative Petrophysical and Seismic Evaluation Technique” (QPSET).

A minimum shale volume is computed using several shale indicators at each depth. These minimum values are further corrected using Clavier et al. (1971), Steiber (1973) and Dresser Atlas (1979) and the average of these values is then selected as the characterizing shale volume for that depth.

Accordingly, Eq. (13) were applied in the same area and compared with the results obtained by QPSET, Abdelrahman et al. (2000) to evaluate the reliability of the equation.

The comparison was made for three wells namely; W78-1 (western side of the area—Fig. 4), GS56-1 (central part of the area—Fig. 5), and NEB81-1 (eastern side of the area—Fig. 6).

Table 5 represents the minimum, maximum and average of the values of shale volume for the six wells, that characterizing the Rudeis Formation in the Northern portion of the Gulf of Suez computed by the program and Eq. (13). Also, Figs. 7–9 illustrate the mode of lateral variation of all average, minimum, and maximum values of shale listed in Table 5.

8. Conclusions

The shaly sand reservoir problem was analyzed by incorporating data from three porosity tools (ρ_b, Δ_t, and ϕ_N) in one formula, in addition to other parameters that are readily available from well log measurements. Considering a more generalized treatment than past models previously listed in Table 1 derived the equation. Application of this equation (Eq. (13)) to field data in an area located in the Northern Gulf of Suez Basin of Egypt shows its validity and reliability for many shaly formations irrespective to the mode of shale distribution. In hydrocarbon-bearing formations, the proposed approach gives reasonable values for shale whereas in gas-bearing formation, another treatment is recommended.

Nomenclature

R_w	Connate water resistivity
SFL	Spherical focused log
CEC	Cation exchange capacity
ϕ_{ND}	Combination of neutron–density log
V_{mat}	Matrix velocity
ϕ_E	The effective porosity
ϕ_D	Density-derived porosity
ρ_b	Bulk density
ρ_{ma}	Matrix fluid density
Δ_t	Transit time
Δ_{tsh}	Shale-matrix transit time
A, B and C	The coefficients of second order equation
QPSET	Quantitative Petrophysical and Seismic Evaluation Technique
R_{mf}	Mud filtrate resistivity
DIL	Dual induction log
SP	Self-potential Log
V_{sh}	Shale volume
ϕ_T	The total porosity
ϕ_N	Neutron porosity
ϕ_S	Sonic-derived porosity
ρ_f	Fluid density
ρ_{sh}	Shale-matrix density
Δ_{tf}	Fluid transit time
Δ_{tma}	Matrix transit time
ϕ_{sh}	Shale porosity

Acknowledgements

We would like to express our deep thanks and gratitude to the authorities of the Egyptian General Petroleum Company (EGPC) and the Gulf of Suez Petroleum Company (GUPCO) for permission to work on the data used to conduct this work. Special thanks are also due to Professor Dr. Gotze Tenchov, Department of Meteorology and Geophysics, Faculty of Physics, Sofia University for his valuable scientific comments and stimulating discussions.

References

Abdelrahman, E.M., Kamel, M.H., Bayoumi, M.A., 2000. QPSET: a program for computing reservoir parameters in marginal hydrocarbon zones. Application to the Rudeis section, Gulf of Suez Basin, Egypt. Petrophysics (formerly the Log Analysts) 41 (2), 148–159 (March–April).

Asquith, G.B., Gibson, C., 1982. Basic Well Log Analysis for Geologists: Textbook AAPG, Tulsa, OK, USA. 216 pp.

Clavier, C., Hoyle, W.R., Meunier, D., 1971. Quantitative interpretation of TDT logs: Parts I and II. J. Pet. Technol. 23, 743–763.

Dresser Atlas, 1979. Log Interpretation Charts. Dresser Industries, Houston, TX. 107 pp.

Dresser Atlas, 1983. Log Interpretation Charts. Dresser Ind. 149 pp.

Fertl, W.H., 1987. Log-derived evaluation of shaly clastic reservoirs. J. Pet. Technol. 39, 175–194.

Hilchie, D.W., 1978. Applied Open Hole Log Interpretation. D.W. Hilchie, Golden, CO.

Kamel, M.H., Helmi, A., Bayoumi, A.I., 1996. A new theoretical technique for evaluating reservoir parameters in shaly-sand section. Application in an area in the Northern Gulf of Suez of Egypt: A Case History: The 2nd Well Logging Symposium of Japan, September 26–27. Paper A.

Poupon, A., Gaymard, R., 1970. The evaluation of clay content from logs. 11th Ann. Soc. Prof. Well Log Analysts Logging symposium, Los Angeles. Paper G.

Ransom, R.C., 1977. Methods based on density and neutron well logging responses to distinguish characteristics of shaly sandstone reservoir rocks. Log Anal. 18 (3), 47.

Ruhovets, N., 1990. A log analysis technique for evaluating laminated reservoirs in the Gulf Coast area. Log Anal. 31 (5), 294–303.

Schlumberger, 1969. Log Interpretation Charts. Schlumberger Well Services, Houston.

Schlumberger, 1972. Log Interpretation: Volume 1—Principles. Schlumberger Well Services, Houston.

Schlumberger, 1975. A guide to Wellsite Interpretation of the Gulf Coast. Schlumberger Well Services, Houston. 85 pp.

Steiber, R.G., 1973. Optimization of shale volumes in open hole logs. J. Pet. Technol. 31, 147–162.

Tenchov, G.G., 1998. Evaluation of electrical conductivity of shaly sands using the theory of mixtures. J. Pet. Sci. Eng. 21, 263–271.

Waxman, W.H., Smits, L.J.M., 1968. Electrical conductivities in oil-bearing shaly sands. Trans. AIME (SPE) 243, 107–122.

Worthington, P.F., 1985. The evaluation of shaly-sand concepts in reservoir evaluation. Log Anal. 26, 23–40.